Neuropeptides 76 (2019) 101934

Contents lists available at ScienceDirect

Neuropeptides

journal homepage: www.elsevier.com/locate/npep

Corticotropin-releasing factor depolarizes rat lateral vestibular nuclear neurons through activation of CRF receptors 1 and 2

Yi Wang[1], Zhang-Peng Chen[1], Zhong-Qin Yang[1], Xiao-Yang Zhang, Jian-Mei Li, Jian-Jun Wang*, Jing-Ning Zhu*

State Key Laboratory of Pharmaceutical Biotechnology and Department of Physiology, School of Life Sciences, Nanjing University, 163 Xianlin Avenue, Nanjing 210023, China

ARTICLE INFO

Keywords:
Corticotropin-releasing factor
Lateral vestibular nucleus
CRF receptor 1
CRF receptor 2
Motor control

ABSTRACT

Corticotropin-releasing factor (CRF) is a neuropeptide mainly synthesized in the hypothalamic paraventricular nucleus and has been traditionally implicated in stress and anxiety. Intriguingly, genetic or pharmacological manipulation of CRF receptors affects locomotor activity as well as motor coordination and balance in rodents, suggesting an active involvement of the central CRFergic system in motor control. Yet little is known about the exact role of CRF in central motor structures and the underlying mechanisms. Therefore, in the present study, we focused on the effect of CRF on the lateral vestibular nucleus (LVN) in the brainstem vestibular nuclear complex, an important center directly contributing to adjustment of muscle tone for both postural maintenance and the alternative change from the extensor to the flexor phase during locomotion. The results show that CRF depolarizes and increases the firing rate of neurons in the LVN. Tetrodotoxin does not block the CRF-induced depolarization and inward current on LVN neurons, suggesting a direct postsynaptic action of the neuropeptide. The CRF-induced depolarization on LVN neurons was partly blocked by antalarmin or antisauvagine-30, selective antagonists for CRF receptors 1 (CRFR1) and 2 (CRFR2), respectively. Furthermore, combined application of antalarmin and antisauvagine-30 totally abolished the CRF-induced depolarization. Immunofluorescence results show that CRFR1 and CRFR2 are co-localized in the rat LVN. These results demonstrate that CRF excites the LVN neurons by co-activation of both CRFR1 and CRFR2, suggesting that via the direct modulation on the LVN, the central CRFergic system may actively participate in the central vestibular-mediated postural and motor control.

1. Introduction

Corticotropin-releasing factor (CRF) is a 41-amino acid peptide hormone and neurotransmitter mainly synthesized in the hypothalamic paraventricular nucleus (PVN) and has traditionally been implicated in stress and anxiety (Bale and Vale 2004; Deussing and Chen 2018; He et al. 2018; Henckens et al. 2016; Vale et al. 1981). These effects are mediated through two cloned G protein-coupled receptors, CRF receptor 1 (CRFR1) and 2 (CRFR2) (Bale and Vale 2004; Fadok et al. 2017; Ramot et al. 2017). Intriguingly, CRFR1 knockout mice not only show an impaired stress response, but also display abnormal locomotor activity in the open field (Timpl et al. 1998). Intracerebroventricular injection of CRF or urocotin-1, a CRF-related peptide, increases locomotor activity (Ramot et al. 2017; Spina et al. 1996; Sutton et al. 1982). In addition, recent studies show that CRF promotes cerebellar motor coordination and rescues ataxic motor deficits (Wang et al. 2017) and depletion of CRFR1 in cerebellar granule cells accelerates Pavlovian associative eye-blink conditioning (Ezra-Nevo et al. 2018), suggesting an active involvement of the central CRFergic system in motor control and motor learning. However, the exact effects of CRF on structures in the central motor system and their underlying neural mechanisms are still largely unknown.

The lateral vestibular nucleus (LVN) is a major nucleus in the central vestibular nuclear complex in the brainstem, an essential center for maintenance of posture and balance. It receives predominantly afferents from the utricle and the saccule and projects to the ipsilateral ventral horn of the spinal cord via the lateral vestibulo-spinal tract (Carleton and Carpenter 1983; Highstein and Holstein 2006). The LVN therefore mainly integrates the information of linear acceleration and gravity's changes of the body to control the vestibulo-spinal reflexes and

* Corresponding authors.
E-mail addresses: jjwang@nju.edu.cn (J.-J. Wang), jnzhu@nju.edu.cn (J.-N. Zhu).
[1] Y.W., Z.-P.C. and Z.-Q.Y. contributed equally to this work.

https://doi.org/10.1016/j.npep.2019.05.005
Received 18 September 2018; Received in revised form 15 May 2019; Accepted 16 May 2019
Available online 20 May 2019
0143-4179/

posture. Retrograde tracing combined with immunohistochemical studies have revealed a moderate dense of CRFergic neurons and fibers originating from the inferior olive (IO) (Cummings 1989; Errico and Barmack 1993; Palkovits et al., 1987) in the LVN, indicating that the CRF may regulate the vestibulo-spinal reflexes and posture via the LVN. Thus, in the present study, using patch clamp recording and immunofluorescence staining, the effect of CRF on LVN neurons and the underlying receptor mechanisms were investigated. The results demonstrate that CRF directly depolarizes and excites the LVN neurons via co-activation of postsynaptic CRFR1 and CRFR2.

2. Materials and methods

2.1. Animals and brain slice preparations

Twenty-six Sprague-Dawley rats aged 12–14 days of either sex (12 females and 14 males) were decapitated under sodium pentobarbital (40 mg/kg) anesthesia. After the brain was quickly removed and placed in ice-cold artificial cerebrospinal fluid (ACSF) consisting of (in mM): 124 NaCl, 2.5 KCl, 1.25 NaH_2PO_4, 1.3 $MgSO_4$, 26 $NaHCO_3$, 2 $CaCl_2$ and 10 d-glucose equilibrated with 95% O_2 and 5% CO_2, coronal brainstem slices (300 μM in thickness) containing the LVN were cut with a vibroslicer (VT 1200 S, Leica, Wetzlar, Germany), according to the rat brain atlas (Paxinos and Watson 2014). The slices were incubated in 95% O_2 and 5% CO_2 oxygenated ACSF at 35 ± 0.5 °C for at least 1 h and then maintained at room temperature. For whole-cell patch clamp recordings, the slices were transferred to a submerged chamber and continuously perfused with 95% O_2 and 5% CO_2 oxygenated ACSF at a rate of 2 ml/min maintained at room temperature. All animal care and experimental procedures complied with the US National Institutes of Health Guide for the Care and Use of Laboratory Animals (NIH Publication 85–23, revised 2011).

2.2. Whole-cell patch clamp recordings

Whole-cell patch clamp recordings were performed as previously described (Zhang et al. 2011; Wang et al. 2017; Ji et al. 2018) on LVN neurons with borosilicate glass pipettes (3–5 MΩ) filled with an internal solution (composition in mM: 140 *K*-methylsulfate, 7 KCl, 2 $MgCl_2$, 10 HEPES, 0.1 EGTA, 4 Na_2-ATP, 0.4 GTP-Tris, adjusted to pH 7.25 with 1 M KOH). During recording sessions, LVN neurons were visualized with an Olympus BX51WI microscope (Olympus, Tokyo, Japan). Patch clamp recordings were acquired with an Axopatch-700B amplifier (Axon Instruments, Foster City, CA) and the signals were fed into a computer through a Digidata-1440A interface (Axon Instruments) for data capture and analysis (pClamp 10.4, Axon Instruments). Neurons were held at a membrane potential of −60 mV and characterized by injection of rectangular voltage pulse (5 mV, 50 ms) to monitor the whole-cell membrane capacitance, membrane resistance and series resistance. Neurons were excluded from the experiments if the series resistance was not stable or exceeded 20 MΩ.

The slices were bathed with CRF (100–1000 nM; Millipore, Billerica, MA; Cat# 05-23-0050) to stimulate the recorded neurons under current clamp and voltage clamp mode to observe the effect of CRF on membrane potential and whole-cell current, respectively. Tetrodotoxin (TTX; 0.3 μM; Alomone Labs, Jerusalem, Israel; Cat# T-500) was used to determine whether the effect of CRF is postsynaptic. Antalarmin (300 nM; Tocris, Bristol, UK; Cat# 2778) and antisauvagine-30 (aSVG-30, 100 nM; Tocris; Cat# 2071), highly selective antagonists for CRFR1 and CRFR2 respectively, were applied to examine the underlying receptor mechanism. CRF, antalarmin and antisauvagine-30 were all dissolved in DMSO and diluted to the final concentration with fresh ACSF (with 0.1% DMSO in the final concentration), whereas TTX was dissolved directly with ACSF.

Before bath application of each CRFergic compound at known concentrations, the firing rate or membrane potential of the recorded neuron was observed for at least 20 min to assure stability. Then, CRF was added to the perfusing ACSF to stimulate the recorded neuron for a test period of 1 min. After each stimulation, cells were given at least 20 min for recovery and prevention of desensitization. The antagonist was given for at least 15 min before its effect was assessed. Besides the raw data, the inter-spike intervals (ISIs, sampling interval = 1 ms) distributions and the peri-stimulus time histograms (PSTHs) of the recorded neuronal discharges were generated to assess the effects of CRF on the cells.

2.3. Immunofluorescence

Immunofluorescence was performed as previously described (Gao et al. 2017; Wang et al. 2017; Ji et al. 2018). Twelve rats (weighing 150–200 g, 7–8 weeks, 6 males and 6 females) were deeply anesthetized with sodium pentobarbital (65 mg/kg) and perfused transcardially with 100 ml normal saline, followed by 250–300 ml 4% paraformaldehyde in 0.1 M phosphate buffer. Subsequently, the brain was carefully removed, trimmed, and post-fixed in the same fixative for 12 h at 4 °C and then cryoprotected with 30% sucrose for 48 h. Frozen coronal sections (25 μm thick) containing the LVN were obtained by using a freezing microtome (CM 3050S, Leica, Wetzlar, Germany) and mounted on gelatin-coated slides. We rinsed the slices in phosphate buffered saline containing 0.1% Triton X-100 (PBST) and incubated them in 10% normal bovine serum in PBST for 30 min. Sections were incubated overnight at 4 °C with following primary antibody: goat anti-CRFR1 (1:200; Abcam, Cambridge, MA; Cat# ab59023, RRID: AB_941167), rabbit anti-CRFR2 (1:200; Abcam; Cat# ab75168, RRID: AB_1523392) and/or rabbit anti-calbindin (1:1000; Millipore; Cat# PC253L, RRID: AB_213554). After a complete wash in PBS, the sections were incubated in the Alexa 488-conjugated donkey anti-goat IgG (1:2000; Invitrogen, San Diego, CA; Cat# ab150129, RRID: AB_2687506) or Alexa 568-conjugated donkey anti-rabbit IgG (1:2000; Invitrogen; Cat# A10042, RRID: AB_2534017) in room temperature for 2 h. The slides were washed and then mounted in UltraCruz mounting medium containing 4.6-diamidino-2-phenylindole (DAPI) (Santa Cruz Biotechnology, CA, Cat# sc-24,941). DAPI staining was used to identify all cell nuclei. Calbindin marking was applied to stain synaptic boutons that encircled the somata of the LVN large Deiters' neurons (Kevetter, 1996; Puyal et al. 2002; Shaia et al. 2002). Incubations replacing the primary antiserum with control immunoglobulins and/or omitting the primary antiserum were used as negative controls. All micrographs were taken with inverted laser scanning confocal microscope TCS SP8 (Leica). Digital images from the microscope were recorded with LAS X Viewer Software (Leica). For DAPI+, CRFR1+, CRFR2+, CRFR1/CRFR2+ and CRFR1/Calbindin+ quantification, whole tilling LVN images were acquired. Regions of interest were defined based on each individual brainstem tilling image. The threshold values were as follows: Threshold 20%, Seed 10%, and Garbage volume 200. The threshold settings were constant through all the images. Image processing and cell counting was performed with Image Pro Plus 6.0 software (Media Cybernetics, Inc., Rockville, MD) by an investigator who was blind to the group assignments.

2.4. Statistical analysis

All data were analyzed using SigmaPlot 12.5 (Systat Software, San Jose, CA) and expressed as mean ± SEMs. Paired or unpaired 2-tailed Student's *t*-test and one-way analysis of variance (ANOVA) followed by Bonferroni's test were employed for statistical analysis. P-values of < 0.05 were considered to be significant.

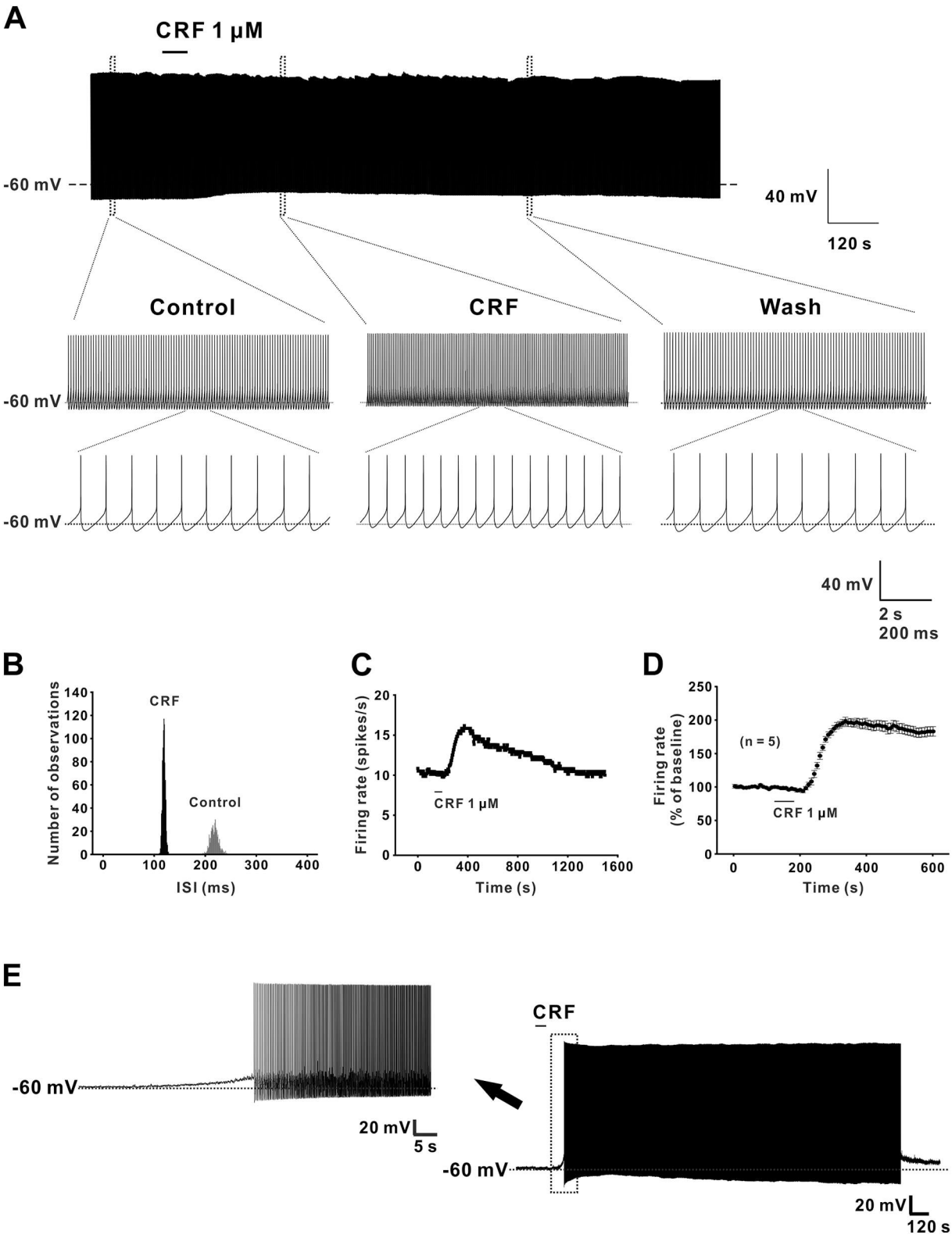

Fig. 1. CRF increases the firing rate of LVN neurons. (A) The effect of CRF (1 min, 1 μM) on a spontaneous firing LVN neuron in current clamp recording. (B) The ISI showed that CRF shortened the inter-spike intervals of the LVN neuron presented in (A). (C) PSTH showed that CRF increased the firing rate of the LVN neuron presented in (A). (D) Group data of 5 recorded spontaneous firing LVN neurons. (E) CRF (1 min, 1 μM) depolarized a silent LVN neuron and evoked the neuron firing. In this and the following figures, the short horizontal bars above the data indicated the 1-min period of application of CRF.

3. Results

3.1. CRF depolarizes and excites LVN neurons

In the present study, a total of 30 LVN neurons with the membrane resistance higher than 150 MΩ were recorded. All of these cells had a whole-cell membrane capacitance > 150 pF and diameter > 30 μM, suggesting that the neurons recorded were giant Deiters' neurons (Li et al. 2017; Uno et al. 2003; Zhang et al. 2008, 2011), whose axons form an important part of the posterior longitudinal bundle that controls the vestibulospinal reflexes. Among the 30 LVN neurons, 17 had spontaneous firing with a mean firing rate of 8.4 ± 0.7 spikes/s and the remaining 13 were silent at rest, consistent with the previous studies that 30–50% neurons in the LVN have no spontaneous discharge (Lai and Chan 2001; Sun et al. 2002; Uno et al. 2003).

We first determined the effect of CRF on firing activities of 10 recorded LVN neurons (5 spontaneous firing and 5 silent) in current clamp recordings. As shown in Fig. 1A, brief bath application (1 min) of CRF (1 μM) increased firing rates of the recorded spontaneous firing LVN neurons from 9.75 ± 1.08 Hz to 15.03 ± 1.35 Hz. Both the ISIs and PSTH of the neurons showed that CRF significantly shortened the intervals of the spikes (Fig. 1B) and increased the firing rates (Fig. 1C). The CRF-induced increment in the peak discharge rates, compared with their basal firing rates, was 99.8 ± 14.1% (n = 5, Fig. 1D). On the other hand, on 5 silent LVN neurons, CRF evoked a strong depolarization response. As shown in Fig. 1E, the magnitude of the CRF-induced depolarization was even sufficient to bring up the neurons firing. These results suggest that CRF excites both spontaneous firing and silent neurons in the LVN.

3.2. The excitation evoked by CRF on LVN neurons is a direct postsynaptic effect

We used TTX to clarify whether the CRF-induced depolarization was a direct postsynaptic effect on 10 LVN neurons (6 spontaneous firing and 4 silent). As shown in Fig. 2A, brief bath application (1 min) of CRF still depolarized LVN neurons in the presence of 300 nM TTX, suggesting a postsynaptic excitatory effect of CRF. Furthermore, CRF induced a postsynaptic depolarization on the LVN neurons in a concentration-dependent manner. Application of 100, 300 and 1000 nM CRF elicited a postsynaptic depolarization of 4.58 ± 0.52 mV, 6.21 ± 0.72 mV and 8.48 ± 0.98 mV, respectively (n = 5, including 3 spontaneous firing and 2 silent neurons, Fig. 2B). Moreover, the voltage clamp recording results showed that bath application of 1 μM CRF induced a stable inward whole-cell current (98.58 ± 7.75 pA, n = 5, including 3 spontaneous firing and 2 silent neurons) in the presence of 300 nM TTX on LVN neurons at the holding potential of −60 mV (Fig. 2C and D), confirming the direct postsynaptic response of CRF on the LVN neurons.

3.3. CRFR1 and CRFR2 co-mediate the CRF-induced excitation on LVN neurons

CRFR1 and CRFR2 selective antagonists were used to determine the receptor mechanism underlying the CRF-induced excitatory response on 10 LVN neurons (6 spontaneous firing and 4 silent). As shown in Fig. 3, in the presence of TTX, highly selective CRFR1 antagonist antalarmin (300 nM) was able to partly block the depolarization response induced by CRF (1 μM) to 62.3 ± 2.4% (n = 5, including 3 spontaneous firing and 2 silent neurons, t = 5.725, df = 4, P = 0.0023, paired t-test, Fig. 3A and C), indicating that CRFR1 receptor is involved in the action of CRF on LVN neurons. The blocking effect of highly selective CRFR2 antagonist aSVG-30 (100 nM) was tested on another 5 LVN neurons as well and the CRF-evoked depolarization was attenuated to 57.9 ± 5.1% (n = 5, including 3 spontaneous firing and 2 silent neurons, t = 6.844, df = 4, P = 0.0024, paired t-test, Fig. 3B and C). Furthermore, co-application of antalarmin (300 nM) and antisauvagine-30 (100 nM), in which 3 neurons (1 spontaneous firing and 2 silent) were firstly perfused with antalarmine and the other 3 neurons (2 spontaneous firing and 1 silent) were firstly applied with antisauvagine-30, totally blocked the depolarization response induced by CRF (1 μM) on LVN neurons (2.7 ± 5.4%, n = 6, t = 11.52, df = 5, P = 0.0003, paired t-test, Fig. 3), strongly suggesting that CRFR1 and CRFR2 co-mediate the excitatory effect of CRF on LVN neurons.

On the other hand, to assess the expression and distribution of CRF receptors in LVN neurons, we performed double immunostaining on the

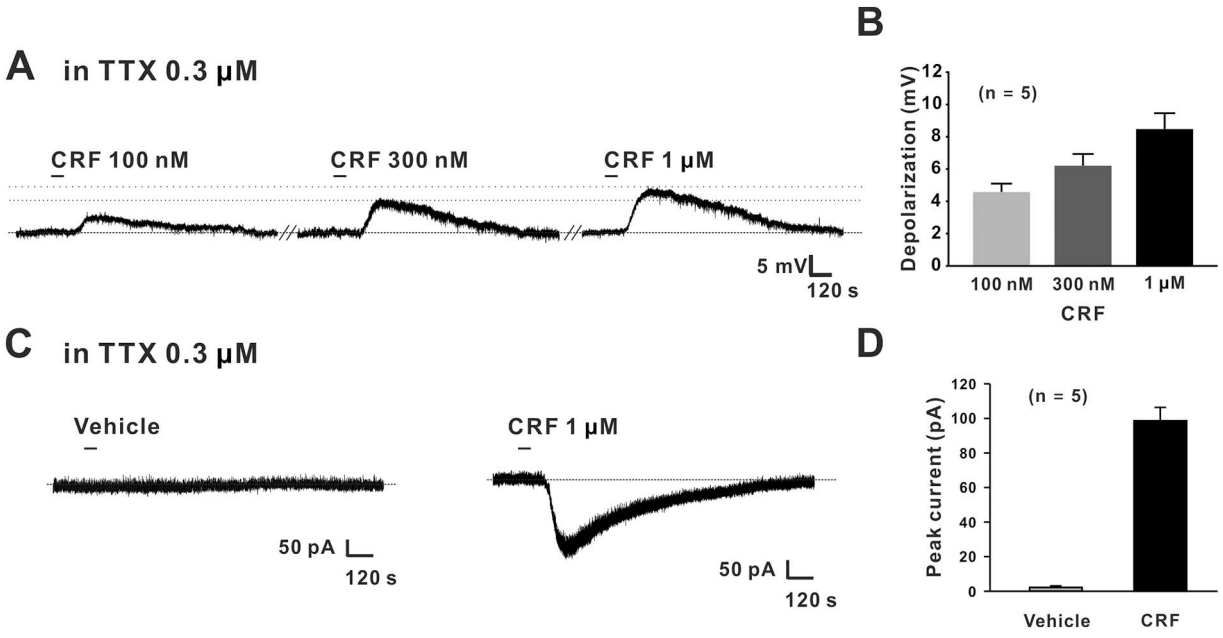

Fig. 2. The depolarization induced by CRF on the LVN neurons is a direct postsynaptic effect. (A) In the presence of TTX, CRF depolarized the LVN neurons in a concentration-dependent manner. (B) Group data of 5 recorded LVN neurons (including 3 spontaneous firing and 2 silent neurons). (C) In voltage clamp recording, TTX did not block the CRF-elicited inward current in a tested LVN neuron. (D) Group data of 5 recorded LVN neurons (including 3 spontaneous firing and 2 silent neurons). Data represent mean ± SEM. Vehicle: 0 0.1% DMSO.

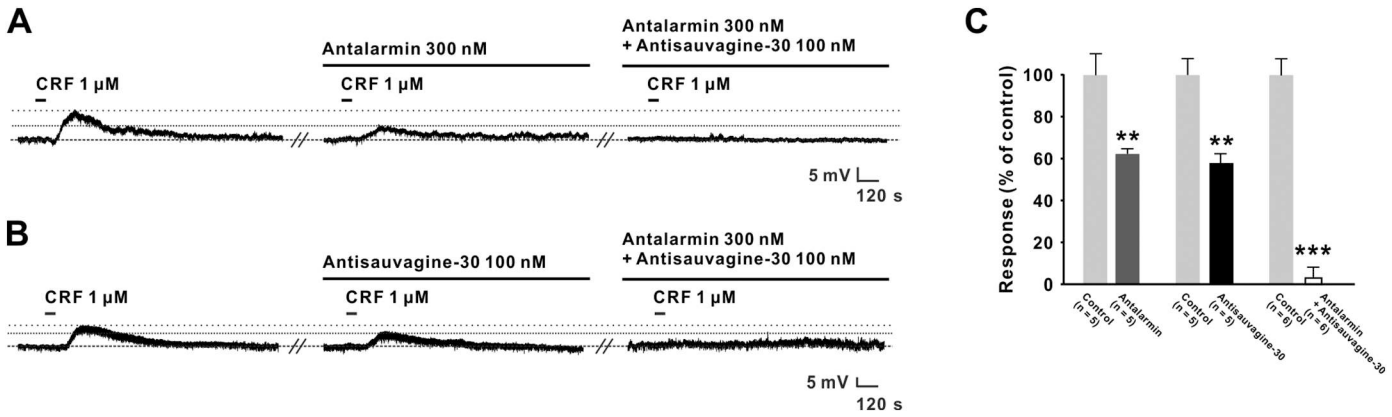

Fig. 3. CRFR1 and CRFR2 co-mediate CRF-induced excitation on the LVN neurons. (A) The CRF-induced depolarization on a tested LVN neuron was partly blocked by antalarmin (300 nM), a highly selective CRFR1 antagonist, and totally abolished by combined application of antalarmin and aSVG-30 (100 nM), a highly selective CRFR2 antagonist. (B) The CRF-induced depolarization on another LVN neuron was partly blocked by aSVG-30, and totally abolished by combined application of antalarmin and aSVG-30. (C) Group data of the recorded LVN neurons (control vs antalarmin, n = 5, including 3 spontaneous firing and 2 silent neurons, $t = 5.725$, df = 4, P = 0.0023, paired *t*-test; control vs aSVG-30, n = 5, including 3 spontaneous firing and 2 silent neurons, $t = 6.844$, df = 4, P = 0.0024, paired t-test; control vs antalarmin in combination with aSVG-30, n = 6, including 3 spontaneous firing and 3 silent neurons, $t = 11.52$, df = 5, P = 0.0003, paired t-test). Data represent mean ± SEM; **P < 0.01, ***P < 0.001, significantly different from the control. In this figure, the long horizontal bars denoted the exposure of the slice to CRF receptor antagonists.

rat brainstem slices containing the LVN with antibodies against CRFR1 and CRFR2 (Fig. 4). The results showed that CRFR1 (Fig. 4B) and CRFR2 (Fig. 4C) were not only present in the rat LVN but also co-localized (Fig. 4D) on the same LVN large cells. The numbers of CRFR1-labeling ($t = 0.4391$, df = 6, P = 0.6760, unpaired Student's t-test), CRFR2-labeling ($t = 0.1761$, df = 6, P = 0.8660, unpaired Student's t-test), and CRFR1/CRFR2 co-labeling cells ($t = 0.8834$, df = 6, P = 0.4110, unpaired Student's t-test) showed no significant difference between males and females (4 rats for each sex and 10 sections for each rat, Fig. 4E), and most of these cells were larger than 30 μM in diameter (referred to as Dieter's cells; Fig. 4F). It has been reported that calbindin forms densely packed heaps of terminal-like structures, which surround LVN large cells (Kevetter, 1996; Puyal et al. 2002; Shaia et al. 2002), calbindin was therefore further chosen as a marker to identify the large Deiters' neurons in the LVN (Fig. 4G-K). Since CRFR1 and CRFR2 were shown to be expressed on the same LVN Deiters' neurons, we next performed double immunostaining with antibodies against calbindin and CRFR1. As shown in Fig. 4G-K, calbindin was strongly labelled encircled the somata of CRFR1 labeling neurons. Moreover, we replaced the primary antiserum and incubated the brain slices contain LVN with control immunoglobulins and/or omitting the primary antiserum. As shown in Fig. 5, no positive signals were detected, indicating the specificity of double labeling performed. These results are consistent with the above-mentioned electrophysiological data and suggest a co-activation of CRFR1 and CRFR2 underlying the CRF-induced excitation on LVN neurons.

4. Discussion

Decreased level of CRF in cerebrospinal fluid was reported in patients with movement disorders, such as Huntington's disease (Desouza et al. 1987), or spinocerebellar and olivopontocerebellar ataxias (Mizuno et al. 1995; Suemaru et al. 1995). Yet little is known about the effect of CRF on central motor structures. Here, in the present study, we report a direct excitatory effect of CRF on neurons in the LVN, a nucleus that directly contributes to adjustment of muscle tone for both postural maintenance and the alternative change from the extensor to the flexor phase during locomotion (De Zeeuw et al., 1994; Garden et al., 2018; Molina-Negro et al., 1980; Wilson and Peterson 1978; Zhang et al., 2017). The central CRFergic system may together with the other neuropeptidergic and monoaminergic systems, such as orexinergic (Zhang et al. 2011), histaminergic (Zhang et al. 2008) and serotonergic (Balaban 2016; Licata et al. 1990), actively modulate central vestibular functions.

Our recent study has revealed that CRF contributes to the control of gait, posture, and motor coordination via exciting projection neurons in the cerebellar nuclei, the ultimate integration and output node of the cerebellum (Wang et al. 2017). Notably, vestibular nuclear complex is the transitional nuclei and an important target for the cerebellar output (Barmack 2003; De Zeeuw and Berrebi 1995; Gao et al., 2012; Voges et al., 2017; Wulff et al., 2009; Yamazaki et al. 2015), which integrates vestibular, visual and motor signals to make compensatory eye and head movements as well as adjustments of muscle tone and posture (Barmack and Yakhnitsa, 2011; De Zeeuw et al., 1997; Highstein and Holstein 2006; Straka et al. 2005; Tokuda et al., 2017). Moreover, elevated levels of CRF in cerebrospinal fluid have been reported in rabbits after optokinetic stimulation (Barmack and Young 1990), indicating that CRF may also be involved in the modulation of neuronal activities of vestibular nuclei. Previous studies have reported that CRF may block the basal chloride permeation across the membranes of LVN Deiters' neurons and this effect can be partially reversed by CRF receptor antagonist (Rapallino et al. 2001). In the present study, we demonstrate for the first time that CRF directly depolarizes and increases the firing rate of LVN Deiters' neurons. Considering that both LVN and cerebellum play critical roles in the control of muscle tone and postural via their descending pathways to the spinal cord, we therefore suggest that the direct and homogeneous excitatory effects of CRF on the LVN and cerebellum may contribute greatly to the vestibular- and cerebellar-related motor reflexes and behaviors.

CRF is a well-known neuropeptide involved in the regulation of stress and anxiety (Anthony et al. 2014; Dabrowska et al. 2016; Deussing and Chen 2018). The interplay between stress responses and vestibular functions has recently received increasing attention. Vestibular nuclei send direct projections to the parabrachial nucleus which has reciprocal relationships with the extended central amygdaloid nucleus, infralimbic cortex, and hypothalamus, constituting the neurological bases for the close association between vestibular balance control and stress response (Balaban 2002; Balaban and Thayer 2001). Considering that the LVN is responsible for vestibulospinal reflexes and postural control (Li et al. 2017; Zhang et al. 2011), fight-or-flight response, which is activated by the sympathetic nervous system and followed by the activation of hypothalamic-pituitary-adrenal axis, may require precise postural and motor control for facing acute stress situations.

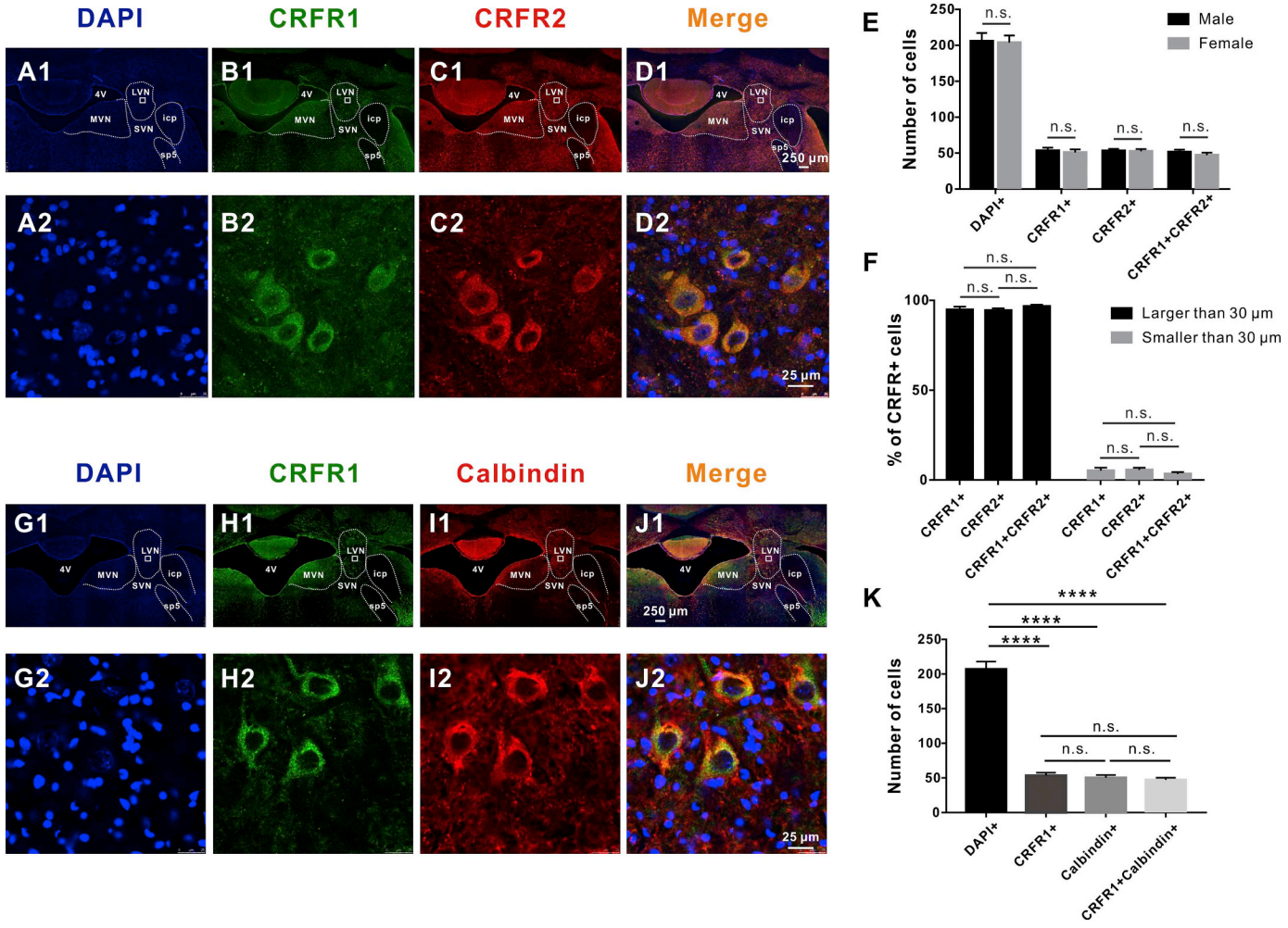

Fig. 4. The distribution of CRFR1 and CRFR2 in the LVN. (A1–D2) Double immunostaining results showed that CRFR1 (B1–B2) and CRFR2 (C1–C2) were not only present in the rat LVN but also co-localized in the same LVN neurons. (E) Cell counts of DAPI+, CRFR1+, CRFR2+ and CRFR1/CRFR2+ neurons both in males and females in the LVN (DAPI+ male vs DAPI+ female, $t = 0.1322$, df = 6, P = 0.8991, unpaired student's t-test; CRFR1+ male vs CRFR1+ female, $t = 0.4391$, df = 6, P = 0.6760, unpaired student's t-test; CRFR2+ male vs CRFR2+ female, $t = 0.1761$, df = 6, P = 0.8660, unpaired student's t-test; CRFR1/CRFR2+ male vs CRFR1/CRFR2+ female, $t = 0.8834$, df = 6, P = 0.4110, unpaired student's t-test). (F) Cell counts of CRFR1+, CRFR2+ and CRFR1+/CRFR2+ neurons larger or smaller than 30 μM in the LVN (Larger than 30 μM: $F_{(2, 9)} = 2.955$, P = 0.1031; CRFR1 vs CRFR2, $t = 0.435$, df = 9, P > 0.9999; CRFR1 vs CRFR1+/CRFR2+, $t = 1.854$, df = 9, P = 0.2902; CRFR2 vs CRFR1+/CRFR2+, $t = 2.289$, df = 9, P = 0.1436, one-way ANOVA followed by Bonferroni's test; Smaller than 30 μM: $F_{(2, 9)} = 2.955$, P = 0.1031; CRFR1 vs CRFR2, t = 0.435, df = 9, P > 0.9999; CRFR1 vs CRFR1+/CRFR2+, t = 1.854, df = 9, P = 0.2902; CRFR2 vs CRFR1+/CRFR2+, t = 2.289, df = 9, P = 0.1436, one-way ANOVA followed by Bonferroni's test). (G1-J2) Double immunostaining results showed that CRFR1 (H1−H2) and calbindin (I1–I2) were co-localized in the same LVN neurons. (K) Cell counts of DAPI+, CRFR1+, Calbindin+ and CRFR1/Calbindin+ neurons in the LVN ($F_{(3, 12)} = 150.7$, P < 0.0001; DAPI+ vs CRFR1+, $t = 17$, df = 12, P < 0.0001; DAPI+ vs Calbindin+, $t = 17.36$, df = 12, P < 0.0001; DAPI+ vs CRFR1/Calbindin+, $t = 17.69$, df = 12, P < 0.0001; CRFR1+ vs Calbindin+, $t = 0.36$, df = 12, P > 0.9999; CRFR1+ vs CRFR1/Calbindin+, $t = 0.6922$, df = 12, P > 0.9999; Calbindin+ vs CRFR1/Calbindin+, $t = 0.3323$, df = 12, P > 0.9999, one-way ANOVA followed by Bonferroni's test). 4 V, 4th ventricle; MVN, medial vestibular nucleus; LVN, lateral vestibular nucleus; SVN, superior vestibular nucleus; sp5, spinal trigeminal tract; icp, inferior cerebellar peduncle. Data represent mean ± SEM; ****P < 0.0001, significantly different between groups; n.s., has no significant different.

In addition, stress may influence central vestibular functions in health and disease through the effects of stress-related neuroactive substances, such as histamine or neurosteroids, on the central vestibular nuclei (Bergquist and Dutia 2006; Saman et al. 2012). A certain amount of glucocorticoid activation appears to be necessary for the appearance of compensatory via increasing intrinsic excitability of ipsilesional vestibular neurons after labyrinthectomy (Cameron and Dutia 1999), but additional immobilization stress impairs vestibular compensation (Yamamoto et al. 2000), the behavioral recovery that takes place after unilateral peripheral vestibular damage (Chen et al. 2019; Lacour et al. 2016). On the other hand, the postural, ocular motor, perceptive and neurovegetative syndromes resulting from unilateral vestibular neurectomy can generate a stress (Bergquist and Dutia 2006; Tighilet et al., 2009). Increased CRF immunoreactivity in the PVN of the hypothalamus has been reported in the unilateral vestibular neurectomy cats (Saman et al. 2012; Tighilet et al., 2009). Moreover, the expression of c-Fos and the level of CRF in the IO are also elevated in the hemilabyrinthectomy rats (Kaufman et al. 1994). Although it is unknown that the role of PVN CRFergic inputs in motor control, blockage of the IO CRFergic inputs in the cerebellar nuclei induces ataxia-like motor dysfunctions (Ruigrok and Voogd, 2000; Wang et al. 2017). Therefore, the CRFergic modulation on the LVN may hold a key position in the vestibular-mediated motor control and compensation as well as participate in stress response, and consequently contribute to somatic-nonsomatic integration (Zhang et al. 2011; Zhu et al. 2006) in response to stress.

In many brain regions, CRFR1 and CRFR2 mediate the same effects of CRF (Lemos et al. 2012; Riegel and Williams 2008; Wang et al.

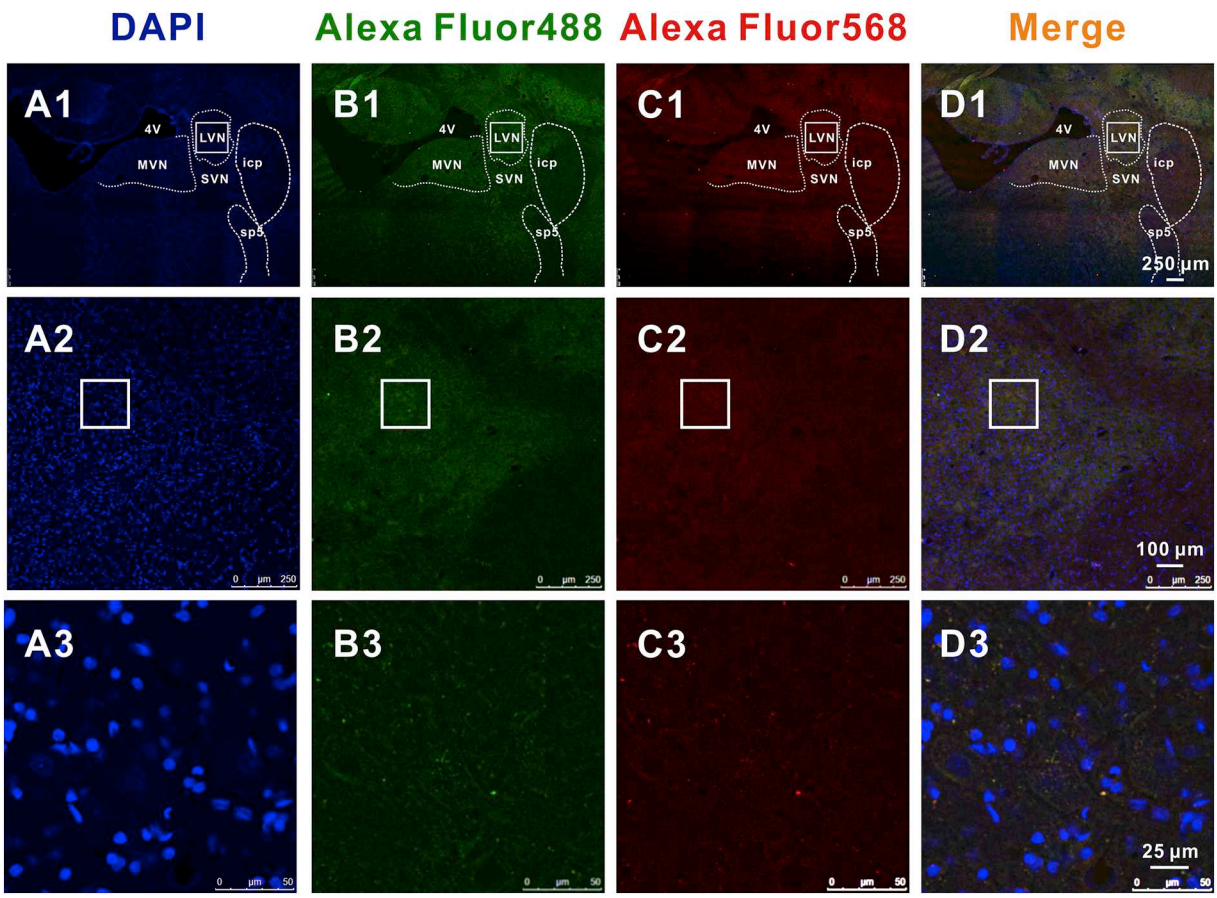

Fig. 5. Neither Alexa Fluor488-labeling nor Alexa Fluor568-labeling neurons are detected in the LVN in negative controls. (A1–D3) Double immunostaining results showed that neither Alexa Fluor488 (B1–B3) nor Alexa Fluor568 (C1–C3) labeling neurons were present in the rat LVN of negative controls, in which the primary antiserum was replaced by control immunoglobulins or omitted. 4 V, 4th ventricle; MVN, medial vestibular nucleus; LVN, lateral vestibular nucleus; SVN, superior vestibular nucleus; sp5, spinal trigeminal tract; icp, inferior cerebellar peduncle.

2017). In the cerebellar nuclei, downregulation or blockage of CRFR1 or CRFR2 induces ataxia-like motor dysfunctions, including gait abnormality, motor incoordination, and postural instability (Wang et al. 2017). Although both CRFR1 and CRFR2 contribute to the CRF-induced excitation on LVN neurons, their specific roles in vestibular functions remain to be elucidated. Moreover, it has been reported that the age and sex influence the expression of CRF receptors in a region-specific manner (Weathington et al. 2014). In the present study, CRFR1 and CRFR2 are expressed in the LVN of both sexes, which is consistent with the previous report that both male and female rats show positive CRF receptor mRNA expression by in situ hybridization (Potter et al. 1994). Since the CRFergic system reaches an adultlike appearance about 2 weeks postnatally in rodents (Cummings et al. 1994) and the LVN neurons can hardly be visualized and recorded in adult rats by patch clamp recordings, we used fortnightly rats in the present electrophysiological experiments. It is furthermore important to determine that whether there are age and/or sex differences in the expression of CRFR in the LVN, the effect of CRF on spontaneous firing and silent LVN neurons, as well as the physiological function of CRF in the LVN circuitry.

In conclusion, the present study reveals a direct excitatory action of CRF on LVN neurons via co-activation of both postsynaptic CRFR1 and CRFR2. Via biasing neuronal activity in the LVN, the central CRFergic system and CRF may be involved in maintaining excitability and setting an appropriate level of sensitivity of LVN for responding to the external vestibular and multisensory information as well as the internal motor signals. Thus, in this way, the central CRFergic system and CRF may actively participate in the regulation of vestibular reflexes and motor control.

Conflict of interests

The authors declare that they have no conflict of interest.

Acknowledgements

This work was supported by the National Natural Science Foundation of China (grants 81671107, 31330033, 31471112, 31600834, and NSFC/RGC Joint Research Scheme 31461163001); the Ministry of Education of China (Fundamental Research Funds for the Central Universities 020814380091); the China Postdoctoral Science Foundation (grant 2017T100351); and Nanjing University Innovation and Creative Program for Ph.D. candidate (grant 2016026).

References

Anthony, T.E., Dee, N., Bernard, A., Lerchner, W., Heintz, N., Anderson, D.J., 2014. Control of stress-induced persistent anxiety by an extra-amygdala septohypothalamic circuit. Cell 156, 522–536. https://doi.org/10.1016/j.cell.2013.12.040.

Balaban, C.D., 2002. Neural substrates linking balance control and anxiety. Physiol. Behav. 77, 469–475. https://doi.org/10.1016/S0031-9384(02)00935-6.

Balaban, C.D., 2016. Neurotransmitters in the vestibular system. Handb. Clin. Neurol. 137, 41–55. https://doi.org/10.1016/B978-0-444-63437-5.00003-0.

Balaban, C.D., Thayer, J.F., 2001. Neurological bases for balance-anxiety links. J. Anxiety. Disord. 15, 53–79. https://doi.org/10.1016/S0887-6185(00)00042-6.

Bale, T.L., Vale, W.W., 2004. CRF and CRF receptors: role in stress responsivity and other behaviors. Annu. Rev. Pharmacol. Toxicol. 44, 525–557. https://doi.org/10.1146/annurev.pharmtox.44.101802.121410.

Barmack, N.H., 2003. Central vestibular system: vestibular nuclei and posterior

cerebellum. Brain Res. Bull. 60, 511–541. https://doi.org/10.1016/S0361-9230(03)00055-8.
Barmack, N.H., Yakhnitsa, V., 2011. Microlesions of the inferior olive reduce vestibular modulation of purkinje cell complex and simple spikes in mouse cerebellum. J. Neurosci. 31, 9824–9835. https://doi.org/10.1523/JNEUROSCI.1738-11.2011.
Barmack, N.H., Young, W.S., 1990. Optokinetic stimulation increases corticotropin-releasing factor messenger-RNA in inferior olivary neurons of rabbits. J. Neurosci. 10, 631–640. https://doi.org/10.1523/JNEUROSCI.10-02-00631.1990.
Bergquist, F., Dutia, M.B., 2006. Central histaminergic modulation of vestibular function - a review. Acta Phys. Sin. 58, 293–304.
Cameron, S.A., Dutia, M.B., 1999. Lesion-induced plasticity in rat vestibular nucleus neurones dependent on glucocorticoid receptor activation. J. Physiol. 518, 151–158. https://doi.org/10.1111/j.1469-7793.1999.0151r.x.
Carleton, S.C., Carpenter, M.B., 1983. Afferent and efferent connections of the medial, inferior and lateral vestibular nuclei in the cat and monkey. Brain Res. 278, 29–51. https://doi.org/10.1016/0006-8993(83)90223-8.
Chen, Z.P., Zhang, X.Y., Peng, S.Y., Yang, Z.Q., Wang, Y.B., Zhang, Y.X., Chen, X., Wang, J.J., Zhu, J.N., 2019. Histamine H1 receptor contributes to vestibular compensation. J. Neurosci. https://doi.org/10.1523/JNEUROSCI.1350-18.2018.
Cummings, S.L., 1989. Distribution of corticotropin-releasing factor in the cerebellum and precerebellar nuclei of the cat. J. Comp. Neurol. 289, 657–675. https://doi.org/10.1002/cne.902890410.
Cummings, S.L., Young, W.S., King, J.S., 1994. Early development of cerebellar afferent systems that contain corticotropin-releasing factor. J. Comp. Neurol. 350, 534–549. https://doi.org/10.1002/cne.903500403.
Dabrowska, J., Martinon, D., Moaddab, M., Rainnie, D.G., 2016. Targeting corticotropin-releasing factor projections from the oval nucleus of the bed nucleus of the stria terminalis using cell-type specific neuronal tracing studies in mouse and rat brain. J. Neuroendocrinol. 28. https://doi.org/10.1111/jne.12442.
De Zeeuw, C.I., Berrebi, A.S., 1995. Postsynaptic targets of Purkinje-cell terminals in the cerebellar and vestibular nuclei of the rat. Eur. J. Neurosci. 7, 2322–2333. https://doi.org/10.1111/j.1460-9568.1995.tb00653.x.
De Zeeuw, C.I., Gerrits, N.M., Voogd, J., Leonard, C.S., Simpson, J.I., 1994. The rostral dorsal cap and ventrolateral outgrowth of the rabbit inferior olive receive a gabaergic input from dorsal group-y and the ventral dentate nucleus. J. Comp. Neurol. 341, 420–432. https://doi.org/10.1002/cne.903410311.
De Zeeuw, C.I., Van Alphen, A.M., Hawkins, R.K., Ruigrok, T.J.H., 1997. Climbing fibre collaterals contact neurons in the cerebellar nuclei that provide a gabaergic feedback to the inferior olive. Neuroscience 80, 981–986. https://doi.org/10.1016/S0306-4522(97)00249-2.
Desouza, E.B., Whitehouse, P.J., Folstein, S.E., Price, D.L., Vale, W.W., 1987. Corticotropin-releasing hormone (CRH) is decreased in the basal ganglia in huntingtons-disease. Brain Res. 437, 355–359. https://doi.org/10.1016/0006-8993(87)91651-9.
Deussing, J.M., Chen, A., 2018. The corticotropin-releasing factor family: physiology of the stress response. Physiol. Rev. 98, 2225–2286. https://doi.org/10.1152/physrev.00042.2017.
Errico, P., Barmack, N.H., 1993. Origins of cerebellar mossy and climbing fibers immunoreactive for corticotropin-releasing factor in the rabbit. J. Comp. Neurol. 336, 307–320. https://doi.org/10.1002/cne.903360211.
Ezra-Nevo, G., Prestori, F., Locatelli, F., Soda, T., ten Brinke, M.M., Engel, M., Boele, H.J., Botta, L., Leshkowitz, D., Ramot, A., Tsoory, M., Biton, I.E., Deussing, J., D'Angelo, E., De Zeeuw, C.I., Chen, A., 2018. Cerebellar learning properties are modulated by the CRF receptor. J. Neurosci. 38, 6751–6765. https://doi.org/10.1523/JNEUROSCI.3106-15.2018.
Fadok, J.P., Krabbe, S., Markovic, M., Courtin, J., Xu, C., Massi, L., Botta, P., Bylund, K., Mueller, C., Kovacevic, A., Tovote, P., Luthi, A., 2017. A competitive inhibitory circuit for selection of active and passive fear responses. Nature 542, 96–100. https://doi.org/10.1038/nature21047.
Gao, Z., van Beugen, B.J., De Zeeuw, C.I., 2012. Distributed synergistic plasticity and cerebellar learning. Nat. Rev. Neurosci. 13, 619–635. https://doi.org/10.1038/nrn3312.
Gao, H.R., Zhuang, Q.X., Zhang, Y.X., Chen, Z.P., Li, B., Zhang, X.Y., Zhong, Y.T., Wang, J.J., Zhu, J.N., 2017. Orexin directly enhances the excitability of globus pallidus internus neurons in rat by co-activating OX1 and OX2 receptors. Neurosci. Bull. 33, 365–372. https://doi.org/10.1007/s12264-017-0127-0.
Garden, D.L.F., Oostland, M., Jelitai, M., Rinaldi, A., Duguid, I., Nolan, M.F., 2018. Inferior olive HCN1 channels coordinate synaptic integration and complex spike timing. Cell Rep. 22, 1722–1733. https://doi.org/10.1016/j.celrep.2018.01.069.
He, F., Ai, H., Wang, M., Wang, X., Geng, X., 2018. Altered neuronal activity in the central nucleus of the amygdala induced by restraint water-immersion stress in rats. Neurosci. Bull. https://doi.org/10.1007/s12264-018-0282-y. Aug 31.
Henckens, M.J.A.G., Deussing, J.M., Chen, A., 2016. Region-specific roles of the corticotropin-releasing factor-urocortin system in stress. Nat. Rev. Neurosci. 17, 636–651. https://doi.org/10.1038/nrn.2016.94.
Highstein, S.M., Holstein, G.R., 2006. The anatomy of the vestibular nuclei. In: Büttner-Ennever, J.A. (Ed.), Neuroanatomy of the Oculomotor syStem, pp. 157–203. https://doi.org/10.1098/rstb.1997.0105.
Ji, M.J., Zhang, X.Y., Peng, X.C., Zhang, Y.X., Chen, Z., Yu, L., Wang, J.J., Zhu, J.N., 2018. Histamine excites rat GABAergic ventral Pallidum neurons via co-activation of H1 and H2 receptors. Neurosci. Bull. 34, 1029–1036. https://doi.org/10.1007/s12264-018-0277-8.
Kaufman, G.D., Anderson, J.H., Beitz, A.J., 1994. Hemilabyrinthectomy causes both an increase and a decrease in corticotropin releasing factor mRNA in rat inferior olive. Neurosci. Lett. 165, 144–148. https://doi.org/10.1016/0304-3940(94)90730-7.
Kevetter, G.A., 1996. Pattern of selected calcium-binding proteins in the vestibular nuclear complex of two rodent species. J. Comp. Neurol. 365, 575–584. https://doi.org/10.1002/(SICI)1096-9861(19960219)365:4<575::AID-CNE5>3.0.CO;2–1.
Lacour, M., Helmchen, C., Vidal, P.P., 2016. Vestibular compensation: the neuro-otologist's best friend. J. Neurol. 263 (Suppl. 1), S54–S64. https://doi.org/10.1007/s00415-015-7903-4.
Lai, C.H., Chan, Y.S., 2001. Spontaneous discharge and response characteristics of central otolith neurons of rats during postnatal development. Neuroscience 103, 275–288. https://doi.org/10.1016/S0306-4522(00)00539-X.
Lemos, J.C., Wanat, M.J., Smith, J.S., Reyes, B.A.S., Hollon, N.G., Van Bockstaele, E.J., Chavkin, C., Phillips, P.E.M., 2012. Severe stress switches CRF action in the nucleus accumbens from appetitive to aversive. Nature 490, 402–406. https://doi.org/10.1038/nature11436.
Li, B., Zhang, X.Y., Yang, A.H., Peng, X.C., Chen, Z.P., Zhou, J.Y., Chan, Y.S., Wang, J.J., Zhu, J.N., 2017. Histamine increases neuronal excitability and sensitivity of the lateral vestibular nucleus and promotes motor behaviors via HCN channel coupled to H2 receptor. Front. Cell. Neurosci. 10, 300. https://doi.org/10.3389/fncel.2016.00300.
Licata, F., Li Volsi, G., Maugeri, G., Santangelo, F., 1990. Effects of 5-hydroxytryptamine on the firing rates of neurons of the lateral vestibular nucleus in the rat. Exp. Brain Res. 79, 293–298. https://doi.org/10.1007/BF00608238.
Mizuno, Y., Takahashi, K., Totsune, K., Ohneda, M., Konno, H., Murakami, O., Satoh, F., Sone, M., Takase, S., Itoyama, Y., Mouri, T., 1995. Decrease in cerebellin and corticotropin-releasing hormone in the cerebellum of olivopontocerebellar atrophy and shy-drager syndrome. Brain Res. 686, 115–118. https://doi.org/10.1016/0006-8993(95)00467-5.
Molina-Negro, P., Bertrand, R.A., Martin, E., Gioani, Y., 1980. The role of the vestibular system in relation to muscle tone and postural reflexes in man. Acta Otolaryngol. 89, 524–533. https://doi.org/10.3109/00016488009127170.
Palkovits, M., Leranth, C., Gorcs, T., Young, W.S., 1987. Corticotropin-releasing factor in the olivocerebellar tract of rats - demonstration by light-microscopic and electron-microscopic immunohistochemistry and insitu hybridization histochemistry. Proc. Natl. Acad. Sci. U. S. A. 84, 3911–3915. https://doi.org/10.1073/pnas.84.11.3911.
Paxinos, G., Watson, C., 2014. The Rat Brain in Stereotaxic Coordinates, Seventh edition. Academic Press/Elsevierhttps://doi.org/10.1016/S0306-4530(03)00088-X.
Potter, E., Sutton, S., Donaldson, C., Chen, R., Perrin, M., Lewis, K., Sawchenko, P.E., Vale, W., 1994. Distribution of corticotropin-releasing factor receptor mRNA expression in the rat brain and pituitary. Proc. Natl. Acad. Sci. U. S. A. 91, 8777–8781. https://doi.org/10.1073/pnas.91.19.8777.
Puyal, J., Devau, G., Venteo, S., Sans, N., Raymond, J., 2002. Calcium-binding proteins map the postnatal development of rat vestibular nuclei and their vestibular and cerebellar projections. J. Comp. Neurol. 451, 374–391. https://doi.org/10.1002/cne.10366.
Ramot, A., Jiang, Z., Tian, J.-B., Nahum, T., Kuperman, Y., Justice, N., Chen, A., 2017. Hypothalamic CRFR1 is essential for HPA axis regulation following chronic stress. Nat. Neurosci. 20, 385–388. https://doi.org/10.1038/nn.4491.
Rapallino, M.V., Cupello, A., Hyden, H., Izvarina, N.L., 2001. Modulation by acute stress of chloride permeation across microdissected vestibular neurons membranes: different results in two rabbit strains and CRF involvement. Brain Res. 890, 255–260. https://doi.org/10.1016/S0006-8993(00)03175-9.
Riegel, A.C., Williams, J.T., 2008. CRF facilitates calcium release from intracellular stores in midbrain dopamine neurons. Neuron 57, 559–570. https://doi.org/10.1016/j.neuron.2007.12.029.
Ruigrok, T.J.H., Voogd, J., 2000. Organization of projections from the inferior olive to the cerebellar nuclei in the rat. J. Comp. Neurol. 426, 209–228. https://doi.org/10.1002/1096-9861(20001016)426:2<209::AID-CNE4>3.0.CO;2-0.
Saman, Y., Bamiou, D.E., Gleeson, M., Dutia, M.B., 2012. Interactions between stress and vestibular compensation - a review. Front. Neurol. 3, 116. https://doi.org/10.3389/fneur.2012.00116.
Shaia, W.T., Shapiro, S.M., Heller, A.J., Galiani, D.L., Sismanis, A., Spencer, R.F., 2002. Immunohistochemical localization of calcium-binding proteins in the brainstem vestibular nuclei of the jaundiced Gunn rat. Hear. Res. 173, 82–90. https://doi.org/10.1016/S0378-5955(02)00631-7.
Spina, M., MerloPich, E., Chan, R.K.W., Basso, A.M., Rivier, J., Vale, W., Koob, G.F., 1996. Appetite-suppressing effects of urocortin, a CRF-related neuropeptide. Science 273, 1561–1564. https://doi.org/10.1126/science.273.5281.1561.
Straka, H., Vibert, N., Vidal, P.P., Moore, L.E., Dutia, M.B., 2005. Intrinsic membrane properties of vertebrate vestibular neurons: function, development and plasticity. Prog. Neurobiol. 76, 349–392. https://doi.org/10.1016/j.pneurobio.2005.10.002.
Suemaru, S., Suemaru, K., Kawai, K., Miyata, S., Nobukuni, K., Ihara, Y., Namba, R., Urakami, K., Hashimoto, K., 1995. Cerebrospinal-fluid corticotropin-releasing hormone in neurodegenerative diseases - reduction in spinocerebellar degeneration. Life Sci. 57, 2231–2235. https://doi.org/10.1016/0024-3205(95)02215-5.
Sun, Y.Z., Waller, H.J., Godfrey, D.A., Rubin, A.M., 2002. Spontaneous activity in rat vestibular nuclei in brain slices and effects of acetylcholine agonists and antagonists. Brain Res. 934, 58–68. https://doi.org/10.1016/s0006-8993(02)02361-2.
Sutton, R.E., Koob, G.F., Lemoal, M., Rivier, J., Vale, W., 1982. Corticotropin releasing-factor produces behavioral activation in rats. Nature 297, 331–333. https://doi.org/10.1038/297331a0.
Tighilet, B., Manrique, C., Lacour, M., 2009. Stress axis plasticity during vestibular compensation in the adult cat. Neuroscience 160, 716–730. https://doi.org/10.1016/j.neuroscience.2009.02.070.
Timpl, P., Spanagel, R., Sillaber, I., Kresse, A., Reul, J., Stalla, G.K., Blanquet, V., Steckler, T., Holsboer, F., Wurst, W., 1998. Impaired stress response and reduced anxiety in mice lacking a functional corticotropin-releasing hormone receptor 1. Nat. Genet. 19, 162–166. https://doi.org/10.1038/520.
Tokuda, I.T., Hoang, H., Kawato, M., 2017. New insights into olivo-cerebellar circuits for

learning from a small training sample. Curr. Opin. Neurobiol. 46, 58–67. https://doi.org/10.1016/j.conb.2017.07.010.
Uno, A., Idoux, E., Beraneck, M., Vidal, P.P., Moore, L.E., Wilson, V.J., Vibert, N., 2003. Static and dynamic membrane properties of lateral vestibular nucleus neurons in Guinea pig brain stem slices. J. Neurophysiol. 90, 1689–1703. https://doi.org/10.1152/jn.00201.2003.
Vale, W., Spiess, J., Rivier, C., Rivier, J., 1981. Characterization of a 41-residue ovine hypothalamic peptide that stimulates secretion of corticotropin and beta-endorphin. Science 213, 1394–1397. https://doi.org/10.1126/science.6267699.
Voges, K., Wu, B., Post, L., Schonewille, M., De Zeeuw, C.I., 2017. Mechanisms underlying vestibulo-cerebellar motor learning in mice depend on movement direction. J. Physiol. 595, 5301–5326. https://doi.org/10.1113/JP274346.
Wang, Y., Chen, Z.P., Zhuang, Q.X., Zhang, X.Y., Li, H.Z., Wang, J.J., Zhu, J.N., 2017. Role of corticotropin-releasing factor in cerebellar motor control and ataxia. Curr. Biol. 27, 2661–2669. https://doi.org/10.1016/j.cub.2017.07.035.
Weathington, J.M., Hamki, A., Cooke, B.M., 2014. Sex- and region-specific pubertal maturation of the corticotropin-releasing factor receptor system in the rat. J. Comp. Neurol. 522, 1284–1298. https://doi.org/10.1016/j.neuroscience.2009.02.070.
Wilson, V.J., Peterson, B.W., 1978. Peripheral and central substrates of vestibulospinal reflexes. Physiol. Rev. 58, 80–105. https://doi.org/10.1007/BF00580836.
Wulff, P., Schonewille, M., Renzi, M., Viltono, L., Sassoe-Pognetto, M., Badura, A., Gao, Z., Hoebeek, F.E., van Dorp, S., Wisden, W., Farrant, M., De Zeeuw, C.I., 2009. Synaptic inhibition of purkinje cells mediates consolidation of vestibulo-cerebellar motor learning. Nat. Neurosci. 12, 1042–U1118. https://doi.org/10.1038/nn.2348.
Yamamoto, T., Yamanaka, T., Matsunaga, T., 2000. The effect of stress application on vestibular compensation. Acta Otolaryngol. 120, 504–507.
Yamazaki, T., Nagao, S., Lennon, W., Tanaka, S., 2015. Modeling memory consolidation during posttraining periods in cerebellovestibular learning. Proc. Natl. Acad. Sci. U. S. A. 112, 3541–3546. https://doi.org/10.1073/pnas.1413798112.
Zhang, J., Han, X.H., Li, H.Z., Zhu, J.N., Wang, J.J., 2008. Histamine excites rat lateral vestibular nuclear neurons through activation of post-synaptic H2 receptors. Neurosci. Lett. 448, 15–19. https://doi.org/10.1016/j.neulet.2008.10.027.
Zhang, J., Li, B., Yu, L., He, Y.C., Li, H.-Z., Zhu, J.N., Wang, J.J., 2011. A role for orexin in central vestibular motor control. Neuron 69, 793–804. https://doi.org/10.1016/j.neuron.2011.01.026.
Zhang, Y., Zhang, Z., Xiao, S., Tien, J., Le, S., Le, T., Jan, L.Y., Yang, H., 2017. Inferior olivary tmem16b mediates cerebellar motor learning. Neuron 95, 1103–1111. https://doi.org/10.1016/j.bpj.2017.11.752.
Zhu, J.N., Yung, W.H., Kwok-Chong Chow, B., Chan, Y.S., Wang, J.J., 2006. The cerebellar-hypothalamic circuits: potential pathways underlying cerebellar involvement in somatic-visceral integration. Brain Res. Rev. 52, 93–106. https://doi.org/10.1016/j.brainresrev.2006.01.003.